JOURNAL OF MATERIALS SCIENCE **35** (2000) 1257–1268

Mechanical properties of weakly segregated block copolymers

Part IV *Influence of chain architecture and miscibility on tensile properties of block copolymers*

R. WEIDISCH*
Max-Planck-Institut für Polymerforschung, Postfach 3148, D-55021 Mainz, Germany
E-mail: RolandWeidisch@aol.com

G. H. MICHLER
Martin-Luther-Universität Halle-Wittenberg, Institut für Werkstoffwissenschaft, D-06099 Halle, Germany

M. ARNOLD
Martin-Luther-Universität Halle-Wittenberg, Institut für Technische und Makromolekulare Chemie, D-06108 Halle/Saale, Germany

H. FISCHER
TNO Institute of Applied Physics, P.O. Box 595, Eindhoven, The Netherlands

Different types of weakly segregated block copolymers are investigated with respect to the influence of chain architecture and miscibility on tensile properties. Poly(styrene-b-butylmethacrylate) diblock copolymers (PS-b-PBMA) as well as poly(butylmethacrylate-b-polystyrene-b-butylmethacrylate) triblock copolymers (PBMA-b-PS-b-PBMA) show synergistic effects on tensile properties. The triblock copolymers show a higher tensile strength and stiffness compared to that of the diblock copolymers. In addition, the triblock copolymers exhibit a larger composition range for which the tensile strength exceeds that of the respective homopolymers. In order to investigate the influence of block miscibility on tensile properties, poly(methylmethacrylate-b-butylmethacrylate) diblock copolymers (PMMA-b-PBMA) are compared with PS-b-PBMA diblock copolymers.

1. Introduction

A vigorously evolving and highly interdisciplinary area of research in last decades has been the emerging field of block copolymers. Much efforts has been made to optimize polymer properties to design materials for a specific use. To provide particular mechanical properties, the use of block copolymers opens a wide field of possibilities due to different available microphase separated morphologies.

The enhancement of toughness in rubber modified materials or polymer blends depends on their morphology. It is well known that the impact properties of homopolymers can be improved by the incorporation of a dispersed elastomeric phase which is due to multiple crazing or multiple cavitation with shear yielding, macroscopically shown by the phenomenon of stress-whitening [1, 2].

In contrast to polymer blends, block copolymers form various ordered morphologies in a size scale of typically 10–100 nm. Block copolymers show usually a macroscopic grain structure in the size scale of 1–10 μm. Such materials exhibit isotropic properties in the absence of macroscopic orientations. In poly(styrene-b-isoprene), (PS-b-PI) diblock copolymers the following morphologies have been reported: BCC-spheres, hexagonally packed cylinders, ordered bicontinuous double diamond (OBDD) and lamellar structures [3–6]. In the weak segregation limit the perforated layer and the cubic bicontinuous structures ("gyroid") have been found [7–9]. Recently, Stadler *et al.* [10–12] have reported new morphologies in ABC block copolymers consisting of three different components (e.g. PS-b-PB-b-PMMA), demonstrating the complexity of structure formation of block copolymers compared to other polymeric systems.

Most block copolymer studies have been focused on morphology and phase behavior. Many authors investigated the phase behavior, morphologies, and mechanical properties of block copolymers consisting of PS and PB or PI. PS-b-PB-b-PS triblock copolymers, such

* corresponding author

as Kratons®, are commonly used thermoplastic elastomers (TPE) [13]. TPE's consist of a hard block (crystalline or glassy) and a rubbery soft block. The TPE Kraton® (Shell Oil Co.) is such a material consisting of a glassy PS block and a rubbery PB middle block [13, 14]. It is best known for the unique thermomechanical properties associated with a phase morphology of PS domains dispersed in a continuous rubbery PB matrix. Whereas PS-b-PB diblock copolymers show only a very small tensile strength, the presence of bridged midblock conformations in PS-b-PB-b-PS (SBS) triblock copolymers provide an improved mechanical strength. The deformation behaviour of the PS-cylinders in SBS triblock copolymers at higher strains has been intensively investigated by various methods [15–18, 19].

In contrast to many other block copolymers, PS-b-PBMA shows a weak segregation at higher molecular weights which allows us to investigate the correlation between phase behavior and mechanical properties in the molecular weight range of $M_n > 200$ kg/mol [20] where the mechanical properties do not show a molecular weight dependence. Russell and co-workers [21, 22] have reported the existence of an upper critical order transition (UCOT) and a lower critical order transition (LCOT) in PS-b-PBMA diblock copolymers. Recently, Ruzette *et al*. [23] have shown that dPS-b-alkylmethacrylate diblock copolymers with long side chain methacrylates $n \geq 6$ reveal an UCOT behavior. In contrast, diblock copolymers with short side chain methacrylates $n < 5$ reveal a LCOT behavior.

Whereas in our previous studies the correlation between morphology, phase behavior, and mechanical properties of PS-b-PBMA diblock copolymers were discussed [24–26], in the present study different weakly segregated block copolymer systems are compared with respect to the influence of chain architecture and miscibility on tensile properties.

2. Experimental

2.1. Polymerization procedure

All polymerizations were carried out in carefully flamed glass reactors in THF at $-78\,^{\circ}$C under an argon atmosphere using syringe techniques. After several cycles of degasing the monomer over calcium hydride, the monomer was introduced into the reactor by condensation under reduced pressure. For PS-b-PBMA and PMMA-b-PBMA diblock copolymers the desired amount of initiator was added at once and after 15 min the living polystyrene or methylmethacrylate anions were end-capped with diphenylethylene. Butyl methacrylate as the second monomer was added dropwise very slowly with a syringe. The living anions were terminated by adding methanol after another 30 min. Then, the polymer was precipitated in a 7/3 methanol/water mixture at $-30\,^{\circ}$C, washed and dried in vacuum for several days.

For PBMA-b-PS-b-PBMA triblock copolymers 1,4-diphenyl-1,4-dilithium was used as bifunctional initiator. After dagasing the styrene was introduced into reactor together with naphthyllithium (*in situ* reaction of naphthylithium to 1,4-diphyenyl-1,4-dilithium). Then the living polystyrene anions were end-capped with diphenyllithium and butyl methacrylate was added dropwise as second monomer as for the diblock copolymers. In contrast to diblock copolymers a bicunctional start of anionic polymerization occurs.

2.2. Sample preparation

All samples were cast from toluene. The solvent was allowed to evaporate slowly over 5–7 days at room temperature. The films were then dried to constant weight in a vacuum oven at 120°C for 3 days for the block copolymers of PS and PBMA. An annealing temperature 140°C was used for the PMMA-b-PBMA block copolymers because of the higher Tg of the PMMA block. The sample preparation method is designed to drive these systems towards equilibrium.

2.3. Characterisation

Molecular weights were determined via Size exclusion chromatography (SEC) using a Knauer-SEC with a RI/Viscodetector and a PS standard linear column.

TABLE I Characterization datas of PS-b-PBMA diblock copolymers (data reproduced from Weidisch *et al*. [25])

Sample	M_n [kg/mol][a] (M_w/M_n)	Φ_{PS}[b]-block	Morphology (TEM)	χN
PBMA	285,0 (1,03)	0	—-	—
SBM 15	406,8 (1,05)	0.15	PS-spheres	38.3
SBM 25	277,0 (1,05)	0.23	PS-cylinder	27.0
SBM 35	270,0 (1,08)	0.35	PS-cylinder	27.2
SBM 39	254,0 (1,05)	0.39	Bicontinuous	25.9
SBM 40	212,1(1,05)	0.40	Perforated lamellae	21.7
SBM 50	278,0 (1,07)	0.51	Lamellae	29.5
SBM 70	286,0 (1,05)	0.70	Lamellae	32.1
SBM 72	426,0 (1,04)	0.72	Lamellae/PBMA-cylinder	48.1
SBM 76	459,0 (1.09)	0.76	PBMA-cylinder	52.4
SBM 83	383,1 (1,04)	0.83	PBMA-spheres	44.6
PS	315,0 (1,02)	1	—	—

Molecular weight (M_n), volume fraction (Φ_{PS}) and polydispersity (M_w/M_n), χN values at 120°C and morphology (TEM) for PS-b-PBMA diblock copolymers used in this study.
[a]Total molecular weights and polydispersity determined by size exclusion chromatography (SEC), values are based on the PS standards.
[b]Volume fraction of PS determined by ^{1}H-NMR.

TABLE II Molecular weight (M_n), volume fraction (Φ_{PS}), polydispersity (M_w/M_n), morphology (TEM), and χN values at 140°C ($\chi = 0.062$ [27]) for PMMA-b-PBMA diblock copolymers

Sample	$10^{-3} \times M_n$[a] copolymer (M_w/M_n)	Φ_{PMMA}[b]	Morphology (TEM)	χN
PBMA	285,0 (1,03)	0	—	—
BMAMMA19	387,6 (1.09)	0.19	PMMA-spheres	182.7
BMAMMA33	426,3 (1.10)	0.33	PMMA-cylinder	210
BMAMMA48	429,7 (1.13)	0.48	Lamellae	225.4
BMAMMA64	277,4 (1.13)	0.64	Lamellae	153.6
BMAMMA71	212,5 (1.11)	0.71	Lamellae	120.4
BMAMMA75	214,0 (1.12)	0.75	PBMA-cylinder	122.8
BMAMMA77	226,7 (1.08)	0.77	PBMA-cylinder	130.9
BMAMMA79	214,2 (1.10)	0.79	PBMA-cylinder	124.5
BMAMMA80	202,6 (1.13)	0.80	PBMA-cylinder	118.2
BMAMMA90	226,3 (1.11)	0.90	PBMA-spheres	136.1
PMMA	205,0 (1.04)	—	—	—

[a]Size exclusion chromatography (SEC), values are based on the PS standards.
[b]^{1}H-NMR.

TABLE III Molecular weight (M_n), volume fraction (Φ_{PS}) and polydispersity (M_w/M_n), χN values at 120°C and morphology (TEM) for PBMA-b-PS-b-PBMA triblock copolymers used in this study

Sample	$10^{-3} \times M_n$[a] copolymer (M_w/M_n)	Φ_{PS}[b]-block	Morphology (TEM)	χN
PBMA	285,0 (1,03)	0	—	—
Tri9	334,0 (1.07)	0.09	PS-spheres	30.8
Tri25	312,3 (1.12)	0.25	PS-cylinder	30.5
Tri37	275,1 (1.08)	0.37	Lamellae	27.9
Tri52	201,1 (1.10)	0.52	Lamellae	21.4
Tri65	305,3 (1.06)	0.65	Lamellae	33.8
Tri72	324,6 (1.09)	0.72	PBMA-cylinder	36.6
Tri80	325,5 (1.12)	0.80	PBMA-spheres	37.6
Tri90	299,2 (1.11)	0.90	PBMA-spheres	35.5
PS	315,0 (1,02)	1	—	—

[a]Size exclusion chromatography (SEC), values are based on the PS standards.
[b]^{1}H-NMR.

The volume fraction of the diblock copolymers were estimated by ^{1}H-NMR. The molecular weights, compositions, morphologies, and χN for each sample are summarized in Tables I–III. The dynamic elastic and loss shear moduli, G' and G'', were determined with a Rheometrics RDAII using the temperature step mode and a frequency of 1 Hz. Ultrathin sections (50 nm) were cut at room temperature in a Ultramicrotome (Reichert) equipped with a glass knife. The polystyrene blocks were stained with RuO_4-vapour. Electron microscopic observations were performed with a BS500 transmission electron microscope (TEM) operated at 80 kV. Tensile tests were performed using a universal testing machine (Zwick 1425) at a strain rate of 1.6×10^{-4} s^{-1} or 5.5×10^{-2} s^{-1}. Tensile specimens had a thickness of about 0.5 mm and a total length of 50 mm. The toughness of the block copolymers was determined as absorbed energy from the stress-strain curves. For each sample and strain rate at least 10 samples were investigated.

3. Experimental results and discussion

3.1. Influence of miscibility: PS-b-PBMA and PMMA-b-PBMA diblock copolymers

3.1.1. Phase behavior

In order to discuss the influence of miscibility on mechanical properties two systems with different interaction parameters between the components were used. The first system is PS-b-PBMA where a partial miscibility is observed. Second, PMMA-b-PBMA diblock copolymers were used which show a stronger incompatibility.

In our previous papers [24–26] we reported the morphology, phase behavior, and tensile properties of PS-b-PBMA diblock copolymers. Here, a partial miscibility is observed by DMA for different compositions. It was shown that only the glass transition temperature (Tg) of the PBMA block is shifted towards higher temperatures and the Tg of the PS block remains approximately at 100°C [25]. This means that an essentially pure PS phase exists together with a PS/PBMA mixed phase. Also for PMMA-b-PBMA a partial miscibility is found with asymmetric phase compositions. Fig. 1

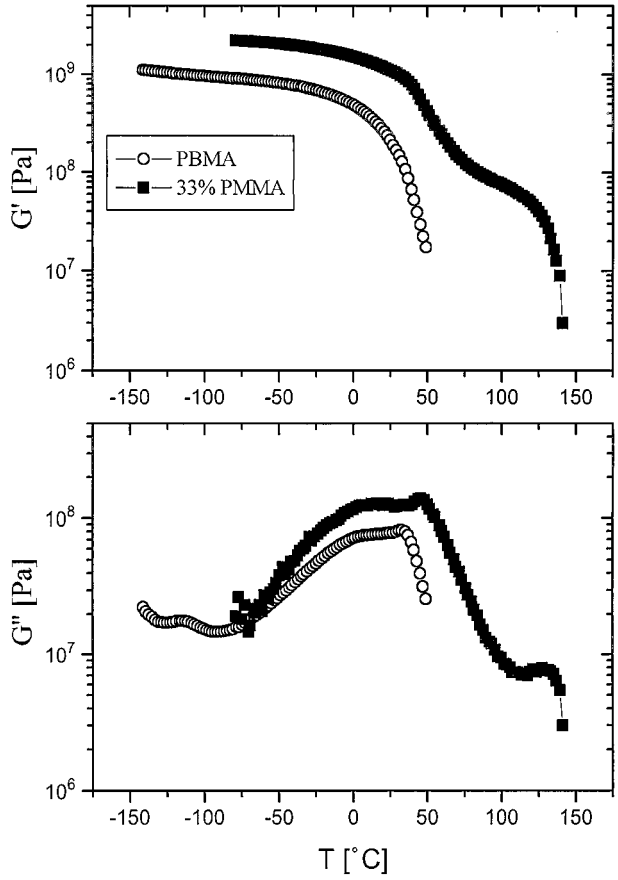

Figure 1 Dependence of storage modulus (G') and loss modulus (G'') on the temperature for a PBMA-b-PMMA diblock copolymer (BMAMMA33: $\Phi_{PMMA} = 0.33$, $M_n = 426$ kg/mol) and pure PBMA (285 kg/mol) measured at a frequency of 1 Hz.

shows the dependence of shear storage (G') and shear loss moduli (G'') on temperature for a PMMA-b-PBMA diblock copolymer with 33% PMMA and 426 kg/mol. It is shown that only the Tg of the PBMA block, indicated by the maximum in G'' modulus, is shifted towards higher temperatures. This leads to the conclusion that also PMMA-b-PBMA diblock copolymers show a partial miscibility.

Small angle neutron scattering (SANS) and neutron reflectometry (NR) can be used to determine the interaction parameter, χ, and interfacial width for both systems. Recently, the temperature dependence of χ for PS-b-PBMA diblock copolymers was determined by SANS to $\chi = (0.0243 \pm 0.0004) - (4.56 \pm 0.169)/T$ [27]. χ increases with increasing temperatures indicating a LCOT behavior. The UCOT, observed by Russell *et al.* [21] can be only found upon heating and will be discussed in ref. [28]. It was shown [29] that between the weak and strong segregation limits an intermediate segregation regime (ISR) between $12.5 < \chi N < 95$ exists where the interface is relatively broad and the junction points are not completly localized in the interfacial region [30]. It is obvious in table I that PS-b-PBMA diblock copolymers are intermediately segregated which was already discussed previously [26, 27]. As shown in Table II, PBMA-b-PMMA diblock copolymers show a larger incompatibility expressed by the relatively large values of χN ($\chi_{PMMA/PBMA} = 0.062$ at $T = 140$°C [31]). While symmetric PMMA-b-PBMA diblock copolymers are strongly segregated, for

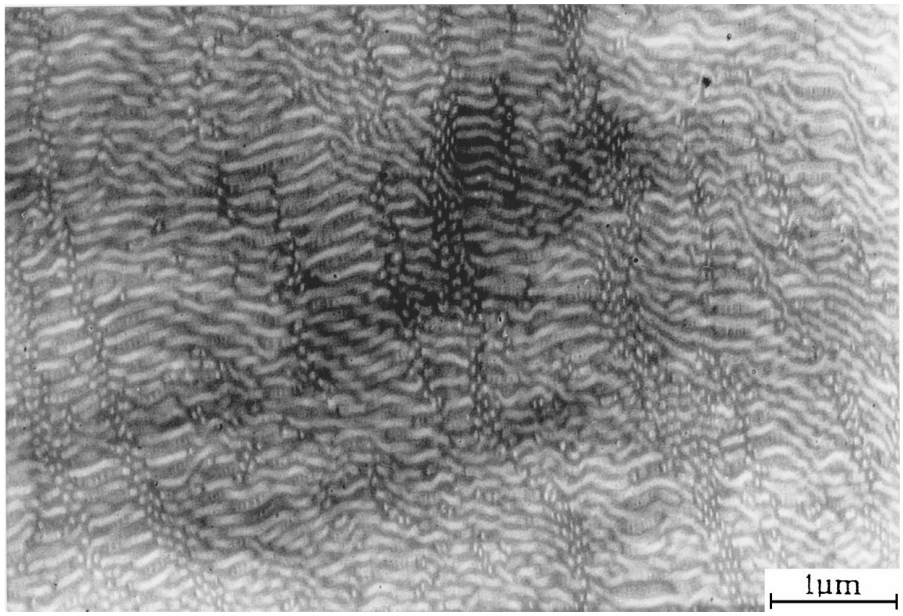

Figure 2 TEM micrograph of hexagonal structure of a PBMA-b-PMMA diblock copolymer (BMAMMA33: $\Phi_{PMMA} = 0.33$, $M_n = 426$ kg/mol (stained with RuO_4: PMMA appears light due to electron beam demage).

asymmetric compositions $(\chi N)_c$ increases which leads to the conclusion that these block copolymers are intermediately segregated ($\chi N - (\chi N)_c < 100$); Table II). For strongly segregated block copolymers the theory of Helfand and coworkers [32] assumes that the interface between A and B domains is narrow compared to the domain size. This was confirmed for PS-b-PI diblock copolymers where an interfacial width of about 2 nm was observed [33]. For the intermediately segregated PS-b-PBMA diblock copolymers a large interfacial width of 8.4 nm was determined by NR [27, 34]. In contrast, for PMMA-b-PBMA diblock copolymers a smaller interface width of about 3.5 nm was observed [31]. These results shows clearly that PMMA-b-PBMA diblock copolymers show a larger incompatibility than PS-b-PBMA diblock copolymers.

3.1.2. Morphology

Our previous investigations [24–26] have shown that PS-b-PBMA diblock copolymers with high molecular weights microphase separate into morphologies with spherical, hexagonal (HEX), lamellar, perforated lamellar (HPL) and gyroid structures depending on composition. In contrast to PS-b-PI diblock copolymers, which show HPL and gyroid structures at both sides of the phase diagram, for PS-b-PBMA diblock copolymers these structures are completely missing at the PS-rich side of the phase diagram where a coexistence of ordered areas of lamellae and hexagonally packed PBMA cylinders (LAM/HEX) exist instead. This indicates an asymmetrical phase diagram for PS-b-PBMA diblock copolymers as discussed elsewhere [28]. In contrast to PS-b-PBMA diblock copolymers for PMMA-b-PBMA block copolymers HPL, LAM/HEX and bicontinuous structures are not observed. PMMA-b-PBMA diblock copolymers show spherical, hexagonal and lamellar structures depending on the composition. The reason for this observation is the decreased miscibility of PMMA-b-PBMA diblock copolymers compared to that of PS-b-PBMA diblock copolymers. It was shown [3–6] that HPL and gyroid structures exist near the order-disorder transition where the microphases are only weakly segregated.

The investigation of the morphologies of PMMA-b-PBMA diblock copolymers was difficult due to the sensivity of both blocks to decomposition in the electon beam. Fig. 2 shows a hexagonal morphology of a PMMA-b-PBMA diblock copolymer with 33% PMMA and 426 kg/mol. It is obvious in Fig. 3 that the PMMA cylinder are hexagonally packed. Further, it is apparent that the PMMA block appears light mainly due to electron beam demage which is well known for PMMA. A lamellar morphology for a PMMA-b-PBMA diblock copolymer with 48% PMMA and 429 kg/mol is shown in Fig. 4. Lamellar structures were found for PMMA contents up to 71% and hexagonally packed PBMA cylinders in the composition regime 75–80% PMMA. A morphology consisting of hexagonally packed PBMA cylinders is shown in Fig. 5 where the cylinders appear to be dark confirming our assumption that the PMMA phase is more affected by the electron beam than the PBMA block.

3.1.3. Mechanical properties

For PS-b-PBMA diblock copolymers a strong increase in tensile strength with increasing PS-content was found. In contrast to other diblock copolymers we found at 76% PS a maximum in tensile strength, which is about 40% higher than that of pure PS [26]. This synergism in tensile strength was found in the composition range between 70% and 80% PS where LAM/HEX and HEX structures were observed. As shown in Fig. 6 PMMA-b-PBMA diblock copolymers show a maximum in tensile strength at 75% PMMA where a hexagonal structure can be observed. However, in contrast to PS-b-PBMA diblock copolymers the tensile strength exceeds the value of PMMA by only about 15%. Also the strain at break as well as the absorbed energy are generally smaller for PMMA-b-PBMA diblock copolymers. It is obvious in Fig. 7 that the maximum

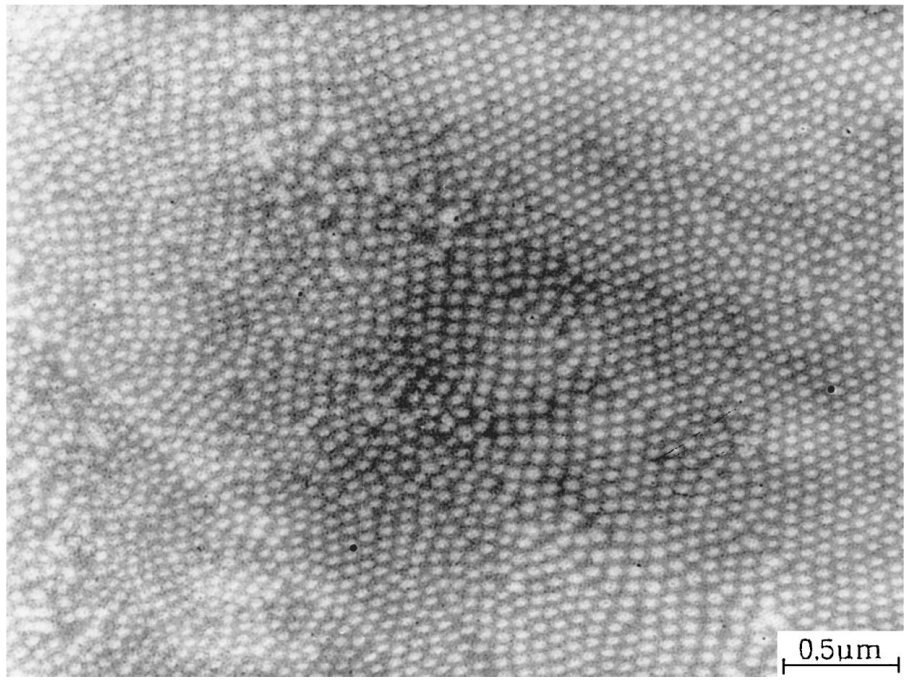

Figure 3 Higher magnification of PBMA-b-PMMA diblock copolymer BMAMMA33 shown in Fig. 2 (stained with RuO_4).

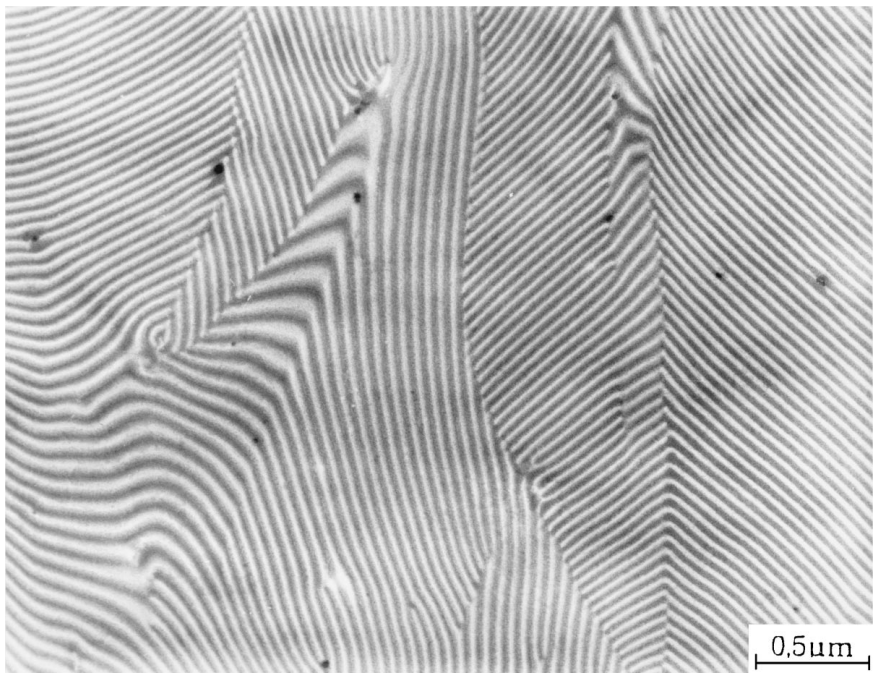

Figure 4 TEM micrograph of lamellar structure of a PBMA-b-PMMA diblock copolymer (BMAMMA48: $\Phi_{PS} = 0.48$, $M_n = 429$ kg/mol; stained with RuO_4. The PMMA lamellae appears light).

of absorbed energy is observed at 19% PMMA where a morphology consisting of PMMA spheres in a PBMA matrix exists. The absorbed energy at this composition exceeds the value of the homopolymers. As already shown in a previous study [25, 26], PS-b-PBMA diblock copolymers also show a synergistic effect in absorbed energy at different strain rates. The absorbed energy shows a maximum in the composition range of 30–40% PS, where hexagonally packed PS-cylinders were found by TEM [25, 26]. This means that the maximum of absorbed energy for PMMA-b-PBMA can be observed at smaller PMMA contents where a spherical morphology is present. Fig. 8 shows the stress-strain curves for PMMA-b-PBMA diblock copolymers with different compositions at a strain rate of $1.6 \times 10^{-4}\,s^{-1}$. At a PMMA content of 75% a transition to brittle behavior occurs corresponding to a transition from lamellar to hexagonal structures as observed by TEM. In contrast, the transition to brittle behavior for PS-b-PBMA copolymers occur at a PS content of 83% corresponding to PBMA spheres [25].

It was shown that most of the important tensile properties such as tensile strength, Young's modulus, and absorbed energy are improved for PS-b-PBMA diblock

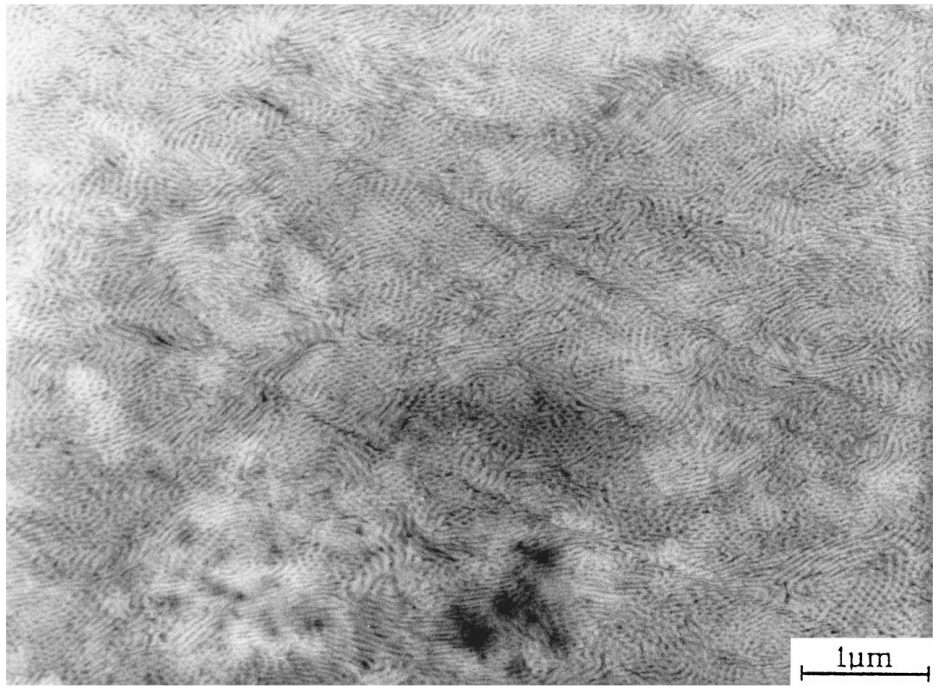

Figure 5 TEM micrograph of a PBMA-b-PMMA diblock copolymer with PBMA cylinder (BMAMMA75: $\Phi_{PMMA} = 0.75$, $M_n = 214$ kg/mol; stained with RuO_4: The PBMA phase appears dark).

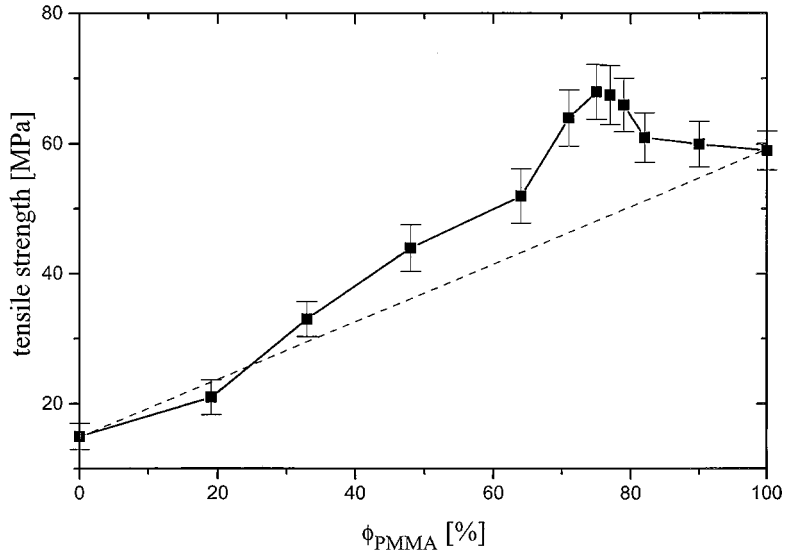

Figure 6 Dependence of tensile strength on volume fraction of PMMA for PMMA-b-PBMA diblock copolymers at a strain rate of $\dot{\varepsilon} = 1.6 \times 10^{-4}\ s^{-1}$.

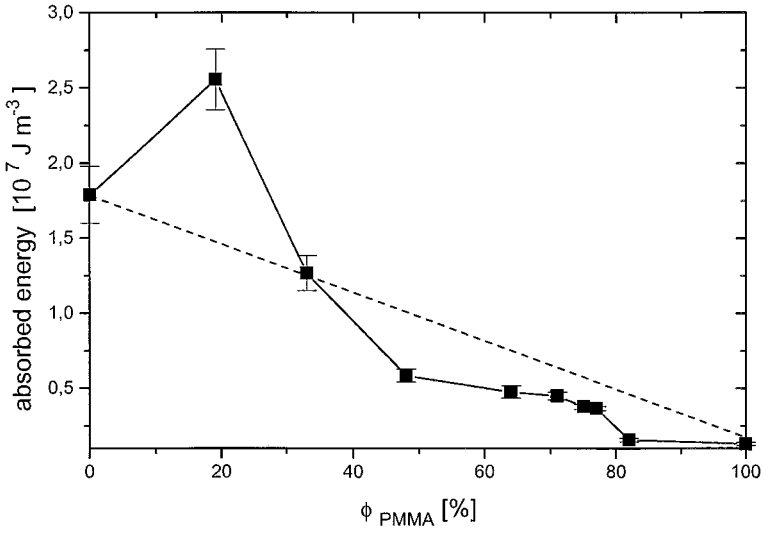

Figure 7 Dependence of absorbed energy on volume fraction of PMMA for PMMA-b-PBMA diblock copolymers at a strain rate of $\dot{\varepsilon} = 1.6 \times 10^{-4}\ s^{-1}$.

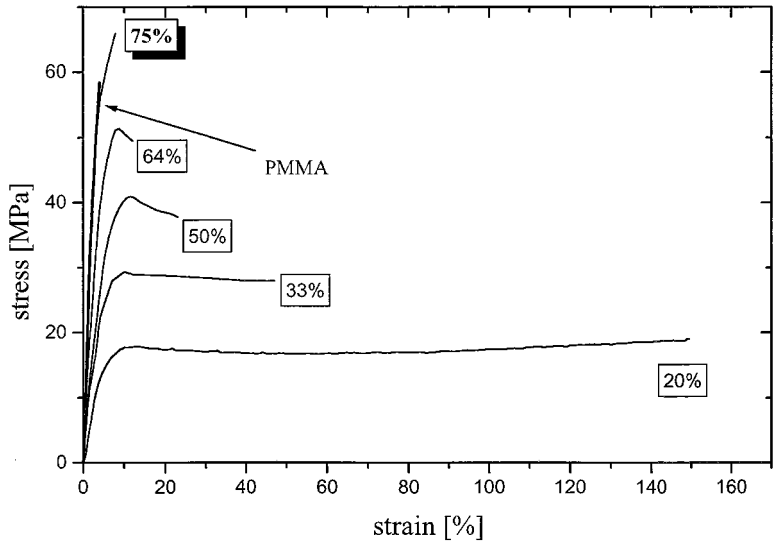

Figure 8 Stress-strain curves for PMMA-b-PBMA diblock copolymers depending on volume fraction of PMMA at a strain rate of $\dot{\varepsilon} = 1.6 \times 10^{-4}\,s^{-1}$.

copolymers compared to that of PMMA-b-PBMA. Our results show that an increasing miscibility leads to improved tensile properties. The broadened interfacial width of PS-b-PBMA diblock copolymers is responsible for their improved tensile strength. It was already discussed in one of our previous papers [27] that an increasing interface width leads to an decreasing stress concentration at the interface resulting in enhanced interfacial strength which is then responsible for the improved tensile strength. Our results are in accordance with observations of Bühler [35] who recognized that a broadened interface in block copolymers can enhance the tensile strength. A statistical PS-co-PI copolymer was introduced as a middle block in PS-b-PI diblock copolymers which leads to an increasing interfacial width and a decrease of domain size. For PS-co-PI contents of about 20% the tensile strength exceeds the value of unmodified PS-b-PI diblock copolymers by about 30% which confirms our result found for weakly segregated block copolymers. It is discussed elsewhere that the partial miscibility of PS-b-PBMA can enhance the craze initiation stress compared to PS [36]. This high values of craze initiation stress provide reasons for the improved tensile strength because crazes are formed at much higher stresses compared to PS-b-PB diblock copolymers.

To explain the improved strains at break and absorbed energy of PS-b-PBMA diblock copolymers the discussion of micromechanical deformation behavior is of great importance. It was shown that in PS-b-PBMA diblock copolymers deformation mechanisms such as diversion of crazes and craze stop exist which are responsible for the improvement of absorbed energies of PS-b-PBMA diblock copolymers [24, 36]. In the case of an broadened interface a large energy dissipation occours at the interface during diversion and stop of crazes and provide reasons for the improved strains at break compared to that of PMMA-b-PBMA diblock copolymers. For PMMA-b-PBMA diblock copolymers at high strain rates of $5.5 \times 10^{-2}\,s^{-1}$ the transition from ductile to brittle behavior occurs already at 64% PMMA where a lamellar morphology is present. This is shown in Fig. 9 for PMMA-b-PBMA where a strong decrease of strain at break occurs compared to the properties at small strain rates. In contrast, for PS-b-PBMA diblock copolymers at the same strain rate this transition was observed at higher PS contents of 76% PS [26]. This means that the properties of PS-b-PBMA

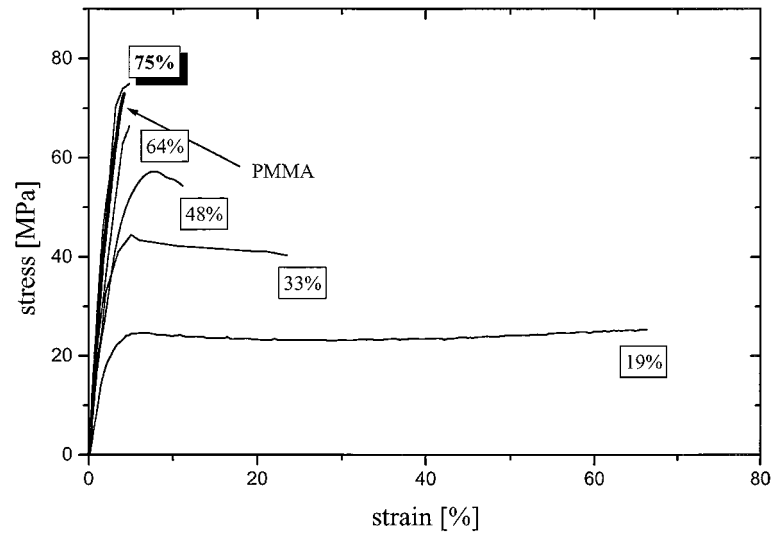

Figure 9 Stress-strain curves for PMMA-b-PBMA diblock copolymers depending on volume fraction of PMMA at a strain rate of $\dot{\varepsilon} = 5.5 \times 10^{-2}\,s^{-1}$.

diblock copolymers are also improved at higher strain rates compared to PMMA-b-PBMA and the phase behavior and interface formation have a pronounced influence on mechanical properties of block copolymers over a wide application range.

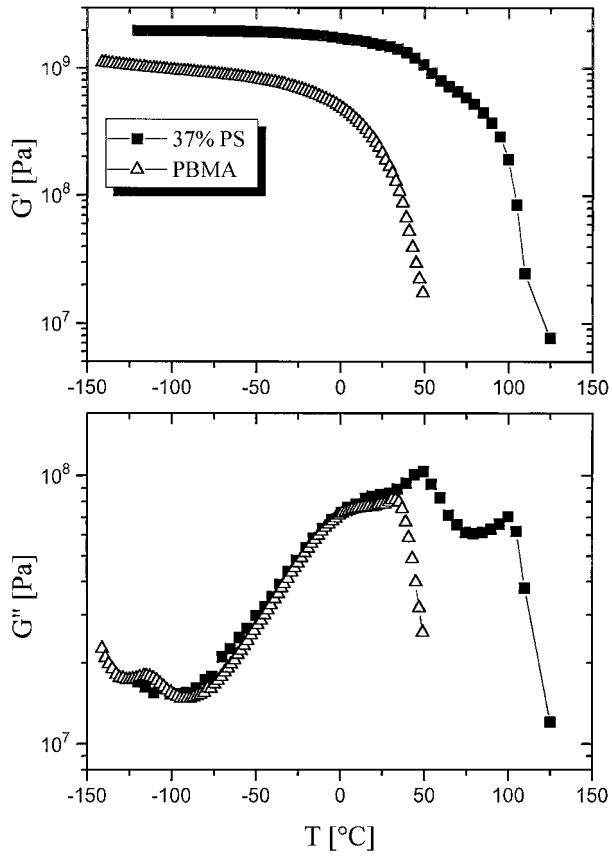

Figure 10 Dependence of storage modulus (G') and loss modulus (G'') on the temperature for a PBMA-b-PS-b-PBMA triblock copolymer (Tri37: $\Phi_{PS} = 0.37$, $M_n = 275$ kg/mole) and PBMA (285 kg/mol) measured at a frequency of 1 Hz.

3.2. Influence of chain architecture: PBMA-b-PS-b-PBMA triblock copolymers

3.2.1. Phase behavior

As with PS-b-PBMA diblock copolymers the triblock copolymers show a partial miscibility where only the Tg of the PBMA-block is shifted to higher temperatures. As shown in Fig. 10, for a triblock copolymer with 37% PS and 275 kg/mol the Tg of the PBMA block is shifted to 50°C which is about 7°C higher than observed for PS-b-PBMA diblock copolymers at the same composition. These observations can be explained by an enhanced miscibility of triblock copolymers compared to that of PS-b-PBMA diblock copolymers. While for diblock copolymers the order-disorder transition is expected at $(\chi N)_c = 10.5$, for triblock copolymers $(\chi N)_c$ increases to 17.9 [37, 38]. In triblock copolymers the presence of two A-B junction points per chain makes the system more compatible than diblock copolymers. Based on the increased value of $(\chi N)_c$ for triblock copolymers one can determine the strength of segregation, $\chi N - (\chi N)_c$, for a triblock copolymer with 52% PS (Table III) to 3.5. This means that the triblock copolymers are weakly segregated. For asymmetric compositions $(\chi N)_c$ increases and the strength of segregation is in the same order.

3.2.2. Morphology

In contrast to PS-b-PBMA diblock copolymers for PBMA-b-PS-b-PBMA triblock copolymers HPL, LAM/HEX and bicontinuous structures are not observed. PBMA-b-PS-b-PBMA triblock copolymers show spheres, cylinders and lamellar structures in the investigated composition regime. Other morphologies may exist in the not investigated composition regime. Fig. 11 shows an example of lamellar structure for a triblock copolymer with 37% PS and 275 kg/mol which is relatively less ordered and quite reminiscent of a

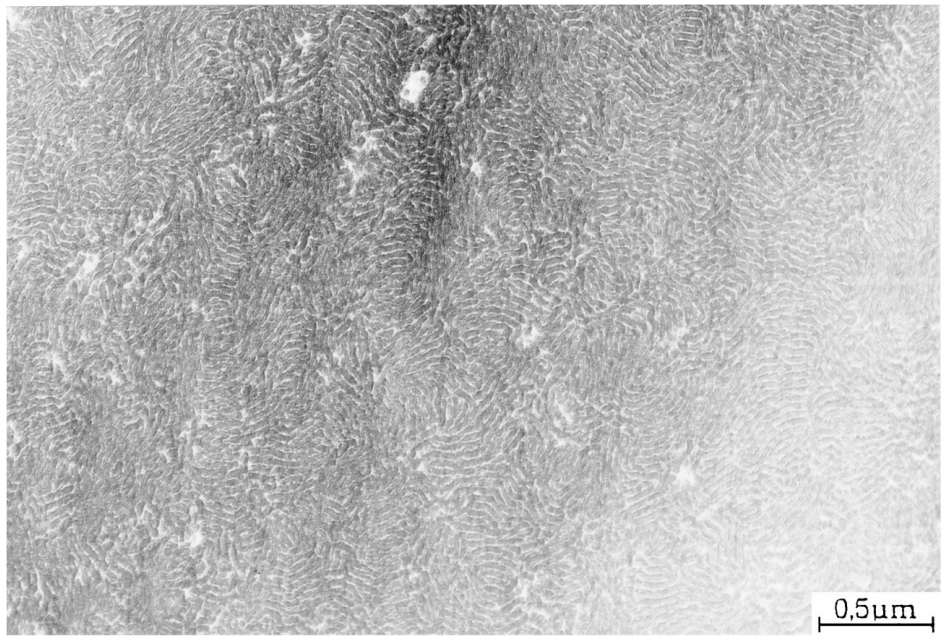

Figure 11 TEM micrograph of lamellar structure of a PBMA-b-PS-b-PBMA triblock copolymer (Tri37: $\Phi_{PS} = 0.37$, $M_n = 275$ kg/mol) with small long range order (stained with RuO4. The PS phase appears dark).

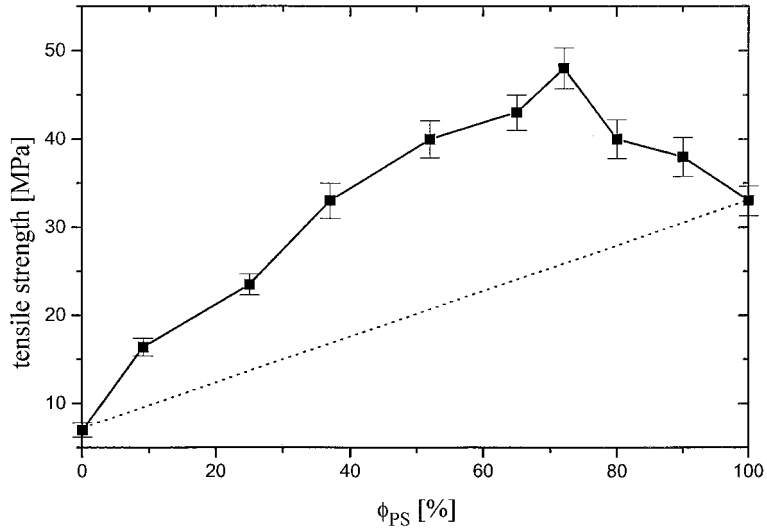

Figure 12 Dependence of tensile strength on volume fraction of PS for PBMA-b-PS-b-PBMA triblock copolymers at a strain rate of $\dot{\varepsilon} = 1.6 \times 10^{-4}\,s^{-1}$.

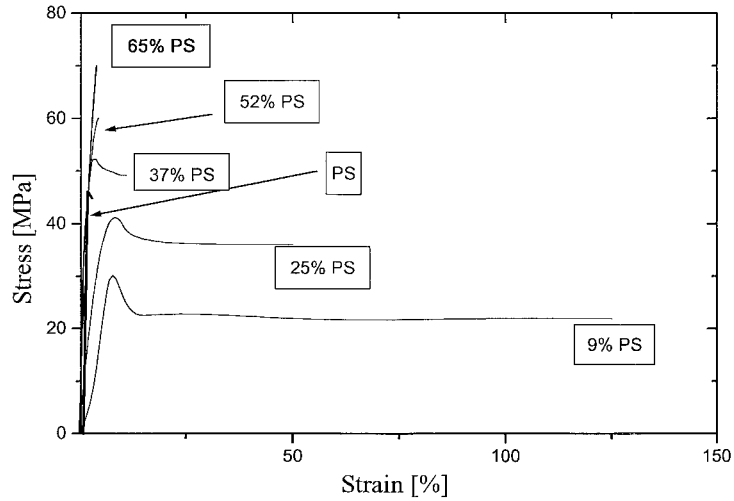

Figure 13 Stress-strain curves for PBMA-b-PS-b-PBMA triblock copolymers depending on volume fraction of PS at a strain rate of $\dot{\varepsilon} = 5.5 \times 10^{-2}\,s^{-1}$.

network-like structure. As already discussed, the triblock copolymers are weakly segregated which is then responsible for the small long range order of the morphology shown in Fig. 11. The morphologies at other compositions are also relatively less ordered and only show small grains. In most block copoly-mers grain structures can be observed in a size scale of 1–10 μm. It is visible in Fig. 11 that only small grains in the size scale of about 200–500 nm exist.

3.2.3. Mechanical properties

As for the diblock copolymers the tensile strength of triblock copolymers strongly increases with increasing polystyrene content (Fig. 12). The tensile strength of polystyrene is already reached at a triblock copolymer composition of 37% PS. At $\Phi_{PS} = 0.72$ a maximum of tensile strength is found, which is also significantly higher than that of polystyrene. The maximum of tensile strength is also observed for a structure consisting of PBMA cylinders in a PS matrix which is already found for diblock copolymers. This morphology seems to be associated with an improved tensile strength.

For triblock copolymers, the synergetic effect in tensile strength exists over a wider composition range than for diblock copolymers. The strain at break is strongly decreased with increasing PS contents (Fig. 13) and is generally smaller than observed for PS-b-PBMA and PMMA-b-PBMA diblock copolymers. This can only be understood, if one assumes that not only the phase behavior, but also the shape of the morphology has an influence on deformation behavior and tensile properties. The less ordered structures in triblock copolymers associated with small grains in a size scale of 200–500 nm have a pronounced influence on tensile properties. Therefore, deformation mechanisms such as craze stop and diversion of crazes can not be observed in triblock copolymers in a large size scale compared to PS-b-PBMA diblock copolymers and improved strains at break are not found. Diversion of crazes and craze stop mechanisms was not observed in triblock copolymers by investigations of deformation behavior using an in-situ tensile device in a high voltage electron microscope (HVEM) [39].

This leads to the conclusion that for improved strains at break and absorbed energies a partial miscibility (intermediate segregation) and quite ordered morphologies with grain structures in a large size scale of 1–10 μm are necessary. While the high tensile strength of triblock copolymers is attributed to the large miscibility

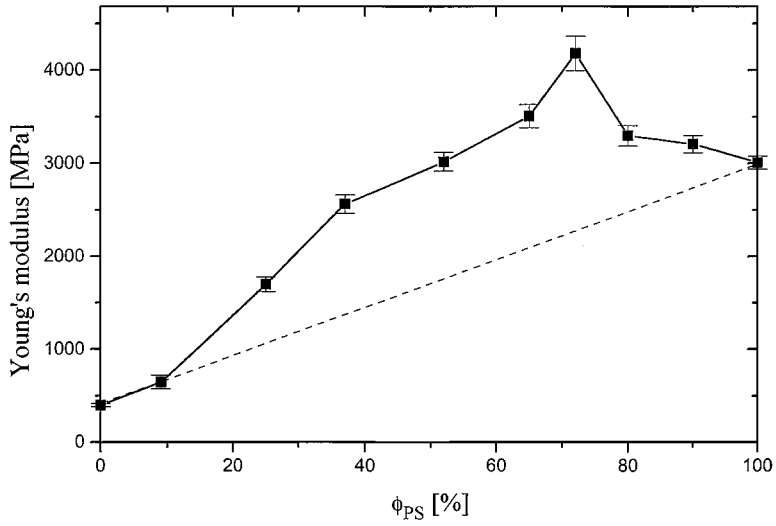

Figure 14 Depencence of Young's modulus on volume fraction of PS for PBMA-b-PS-b-PBMA triblock copolymers.

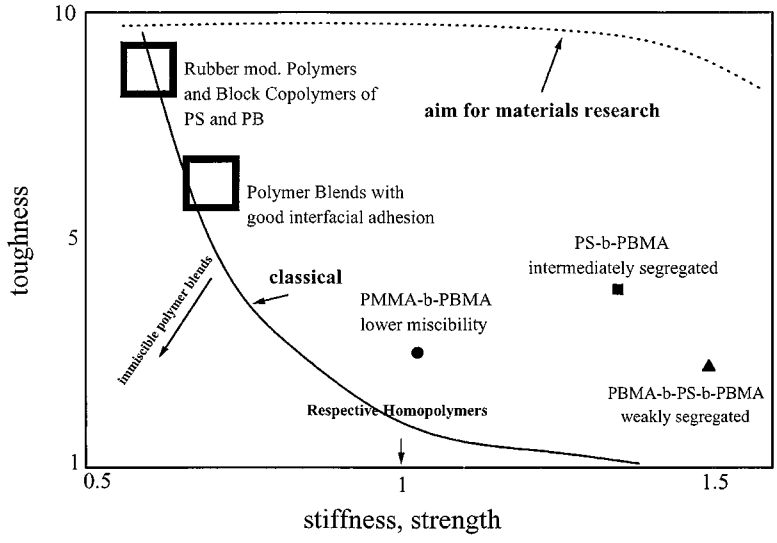

Figure 15 Qualitatively dependence of toughness on tensile strength and stiffness for different polymeric systems which demonstrate the non-classical property profile of weakly segregated block copolymers with different miscibilities.

and broadened interface, the small strains at break are due to the relatively less ordered structures of the weakly segregated triblock copolymers.

This results indicate that not only the phase behavior, but also the long range order of morphology in block copolymers can be correlated to their tensile properties.

Finally, the behavior of weakly segregated block copolymers also seem to have a pronounced influence on stiffness. It was already reported for PS-b-PBMA diblock copolymers, that the Young's modulus exceeds the value of PS by about 20% at a PS content of 76% [26]. For triblock copolymers it is shown in Fig. 14 that the Young's modulus exceeds the value of PS by about 30% and over a larger composition range than that for PS-b-PBMA diblock copolymers. In contrast, for PMMA-b-PBMA diblock copolymers the Young's modulus does not exceed the value of PMMA. These effects are quite complex and therefore relatively less understood.

First, we assume that the Young's modulus can be influenced by the shape of the morphology. It was shown for PS-b-PBMA diblock copolymers [26] that the Young's modulus of the bicontinuous structure is improved compared to that of other morphologies in the composition range of 30–50% PS. This indicates that different models for elastic constants of composites (for example Reuss and Takayanagi) models cannot give a reliable description of the properties of weakly segregated block copolymers because they only include the elastic constants of the respective homopolymers, the volume fraction and the Poisson's constant but do not consider the morphologies and chain architectur of the polymers [26, 40]. Second, we have not found neat phases but a mixed phase and a pure matrix phase which leads to problems of the determination of real Young's modulus for each phase. Further, the modulus of structures in the nm-scale could differ from those of bulk materials and the chain architecture in block copolymers (different chain conformations) could also have a pronounced influence on Young's modulus. While highly ordered structures in block copolymers are responsible for an improvement of toughness, a small long range order associated with a network-like shape of morphology (Fig. 11) and the triblock architecture

seems to be associated with an enhancement of stiffness.

4. Conclusions

Our investigations have clearly shown that phase behaviour, microphase separated morphologies in the nm-scale, interface formation and chain architecture have a pronounced influence on mechanical properties of block copolymers.

It is shown that a decrease of miscibility and interfacial width in the case of PBMA-b-PMMA lead to an deterioration of tensile properties compared to that of PS-b-PBMA diblock copolymers. In contrast, for PBMA-b-PS-b-PBMA triblock copolymers the tensile strength as well as stiffness are improved compared to that of diblock copolymers, demonstrating the influence of chain architecture on tensile properties. However, for triblock copolymers the strains at break are generally smaller than observed for the diblock copolymers.

The large miscibility (small interaction parameter) of weakly segregated block copolymers is associated with a large interfacial width and asymmetrical phase compositions which provide reasons for synergistic effects on tensile properties of weakly segregated block copolymers. Further, it is found that the shape of morphology and their long range order seems to influence the strains at break (toughness). The stiffness of block copolymers seems to be influenced by chain architecture (type of chain conformation) and morphology.

As qualitatively shown in Fig. 15 the most of interesting tensile properties of weakly segregated block copolymers such as tensile strength, stiffness and toughness are improved compared to that of homopolymers which is usually not observed for rubber toughened polymers and most of polymer blends. While the properties of multicomponent polymer systems fullfil the classical correlation between toughness, strength, and stiffness, for weakly segregated block copolymers interesting non-classical correlations are observed. This leads to the assumption that block copolymers can show a new combination of properties which can be controlled by composition, morphology (shape and long range order), phase behavior (state of segregation), interface formation, chain architecture (diblock or triblock), and deformation mechanisms.

Acknowledgement

It is our pleasure to thank Priv.-Doz. Dr. M. Stamm (MPI Mainz), Prof. R. Stadler (†), Dr. V. Abetz (Bayreuth), Prof. V. Altstädt (Hamburg), Dr. D. W. Schubert (GKSS Geesthacht), Prof. E. Donth (Halle), Prof. E. Straube (Halle), Prof. Jerome (Liege) and Dr. F. Ramsteiner (BASF) for the helpful discussions and fruitful collaborations. The authors thank Mrs. E. Hörig and Mrs. S. Goerlitz (Halle) for the TEM-investigations of some of the diblock copolymers. R. Weidisch acknowledges financial support from Deutsche Forschungsgemeinschaft (DFG) and thanks Dr. C. Honeker (MPI Mainz) for reading this manuscript and many fruitful discussions. We also thank Dr. S. Hofman (Makromolekulare Chemie, Halle) for the syntheses of the block copolymers.

References

1. C. B. BUCKNALL, "Toughned Plastics" (Appl. Sci. Publ. Ltd., London, 1977).
2. G. H. MICHLER, "Kunststoffmikromechanik" (Carl Hanser Verlag, München, Wien, 1992).
3. T. HASHIMOTO, K. YAMASAKI, S. KOIZUMI and H. HASEGAWA, *Macromolecules* **26** (1994) 1562.
4. E. L. THOMAS, D. B. ALWARD, D. J. KINNING, D. C. MARTIN, D. L. HANDLIN and L. J. FETTERS, *ibid.* **20** (1987) 1651.
5. K. I. WINEY, D. A. GOBRAN, Z. XU, L. J. FETTERS and E. L. THOMAS, *ibid.* **27** (1994) 2392.
6. R. J. SPONTAK, S. D. SMITH and A. ASHRAF, *ibid.* **34** (1993) 2233.
7. I. W. HAMLEY, K. A. KOPPI, J. H. ROSEDALE, F. S. BATES, K. ALMDAL and K. MORTENSEN, *ibid.* **26** (1993) 5959.
8. D. A. HADJUK, P. E. HARPER, S. M. GRUNER, C. C. HONEKER, G. KIM, E. L. THOMAS and L. J. FETTERS, *ibid.* **27** (1994) 4063.
9. S. FÖRSTER, A. K. KHANPUR, J. ZHAO, F. S. BATES, I. W. HAMLEY, A. J. RYAN and W. BRAS, *ibid.* **27** (1994) 6922.
10. J. BECKMANN, C. AUSCHRA and R. STADLER, *Macromol. Rapid Commun.* **15** (1994) 67.
11. U. KRAPPE, R. STADLER and I. VOIGT-MARTIN, *Macromolecules* **28** (1995) 4558.
12. R. STADLER, C. AUSCHRA, J. BECKMANN, U. KRAPPE, I. VOIGT-MARTIN and L. LEIBLER, *ibid.* **28** (1995) 3080.
13. G. HOLDEN, in "Thermoplastic Elastomers," edited by N. R. Legge, G. Holden and H. E. Schroeder (Hanser, Muinch, 1987) p. 481.
14. M. MORTON, in "Encyclopedia of Polymer Science and Technology," Vol. 15, edited by M. Bikales (Wiley-Interscience, New York, 1971) p. 508.
15. R. SEGULA and J. PRUD'HOMME, *Macromolecules* **18** (1985) 1295.
16. J. A. ODELL and A. KELLER, *Polym. Eng. Sci.* **17** (1977) 544.
17. T. PAKULA, K. SAIJO, H. KAWAI and T. HASHIMOTO, *Macromolecules* **18** (1985) 1295.
18. J. SAKAMOTO, SAKURAI, K. DOI and S. NOMURA, *ibid.* **26** (1993) 3351.
19. C. C. HONEKER and E. L. THOMAS, *Chemistry of Materials* **6** (1996) 1702.
20. R. WEIDISCH, G. H. MICHLER, M. ARNOLD, S. HOFMANN, M. STAMM and R. JÉRÔME, *Macromolecules* **30** (1997) 8078.
21. T. P. RUSSELL, T. E. KARIS, Y. GALLOT and A. M. MAYES, *Nature* **368** (1994) 729.
22. T. E. KARIS, T. P. RUSSELL, Y. GALLOT and A. M. MAYES, *Macromolecules* **28** (1995) 1129.
23. A. RUZETTE, P. BANERJEE, A. M. MAYES, M. POLLARD, T. P. RUSSELL, R. JEROME, T. SLAWECKI, R. HJELM and P. THIYAGARAJAN, *ibid.* **31** (1998) 8509.
24. R. WEIDISCH, E. H ÖRIG, R. LACH, M. ENβlen, G. H. MICHLER, M. STAMM and R. JÉRÔME, *Polymers for Adv. Technolog.* **9** (1998) 727.
25. R. WEIDISCH, G. H. MICHLER, H. FISCHER, S. HOFMANN, M. ARNOLD and M. STAMM, *Polymer* **40** (1999) 1191.
26. R. WEIDISCH, M. STAMM, G. H. MICHLER, H. FISCHER and R. JÉRÔME, *Macromolecules* **32** (1999) 742.
27. R. WEIDISCH, M. STAMM, M. ARNOLD, H. BUDDE and S. HÖRING, *ibid.* **32** (1999) 3405.
28. H. FISCHER, R. WEIDISCH, M. STAMM, M. ARNOLD and G. H. MICHLER, *ibid.*, submitted.
29. M. W. MATSEN and F. BATES, *ibid.* **29** (1996) 1091.
30. J. MELENKEVITZ and M. MUTHUKUMAR, *ibid.* **24** (1991) 4199.
31. J. SCHERBLE, B. STARK, B. STÜHN J. KRESSLER, D. W. SCHUBERT, H. BUDDE, S. HÖRING, P. SIMON and M. STAMM, *ibid.* **32** (1999) 1859.
32. E. HELFAND and Z. R. WASSERMAN, *ibid.* **9** (1976) 897.

33. H. HASEGAWA, H. TANAKA, K. YAMASAKI and T. HASHIMOTO, *ibid.* **20** (1987) 1651.
34. D. W. SCHUBERT, R. WEIDISCH, M. STAMM and G. H. MICHLER, *ibid.* **31** (1998) 3743.
35. F. BÜHLER, Doctoral dissertation, Freiburg, 1986.
36. R. WEIDISCH, M. ENßLEN, H. FISCHER and G. H. MICHLER, *Macromolecules* **32** (1999) 5375.
37. L. LEIBLER, *ibid.* **13** (1980) 1302.
38. M. D. GEHLSEN, K. ALMDAL and F. S. BATES, *ibid.* **25** (1992) 939.
39. R. WEIDISCH, M. ENENßLEN, G. H. MICHLER, *ibid.* in preparation.
40. I. M. WARD, "Mechanical Properties of Solid Polymers," (John Wiley & Sons Ltd., Chichester, UK).

Received 30 July 1998
and accepted 27 May 1999